Product Datasheet

DsRed Antibody (orb345392)

Catalog Number	orb345392
Category	Antibodies
Description	RFP antibody
Target	DsRed
Clonality	Polyclonal
Species/Host	Rabbit
Isotype	IgG
Conjugation	Unconjugated
Reactivity	Other
Form/Appearance	Liquid (sterile filtered)
Concentration	1.10 mg/mL
Buffer/Preservatives	Preservative: 0.01% (w/v) Sodium Azide. Stabilizer: None; Buffer: 0.02 M Potassium Phosphate, 0.15 M Sodium Chloride, pH 7.2
Purity	This product was prepared from monospecific antiserum by immunoaffinity chromatography using Red Fluorescent Protein (Discosoma) coupled to agarose beads followed by solid phase adsorption(s) to remove any unwanted reactivities. Expect reactivity against RFP and its variants: mCherry, tdTomato, mBanana, mOrange, mPlum, mOrange and mStrawberry. Assay by immunoelectrophoresis resulted in a single precipitin arc against anti-Rabbit Serum and purified and partially purified Red Fluorescent Protein (Discosoma). No reaction was observed against Human, Mouse or Rat serum proteins.

Biorbyt Ltd.
7 Signet Court, Swann Road
Cambridge
CB5 8LA
United Kingdom
Email: info@biorbyt.com, support@biorbyt.com
Phone: +44 (0)1223 859353 | Fax: +1 (415) 651-8558

Biorbyt LLC
68 TW Alexander Drive
Research Triangle Park
Durham
NC 27713-2847
United States
Email: info@biorbyt.com, support@biorbyt.com
Phone: +1 (415) 906-5211 | Fax: +1 (415) 651-8558

Immunogen	The immunogen is a Red Fluorescent Protein (RFP) fusion protein corresponding to the full-length amino acid sequence (234aa) derived from the mushroom anemone Discosoma.
UniProt ID	**Q9U6Y8**
Tested applications	ELISA, FC, IF, IHC, WB
Dilution range	ELISA: 1:20,000 - 1:50,000, FC: 1:200 - 1:2,000, IHC: 1:200-1:2,000, IF: 1:200-1:2,000, WB: 1:1,000 - 1:5,000
Application notes	Polyclonal anti-RFP is designed to detect RFP and its variants. This antibody has been tested by ELISA, western blot, IF, and IHC, and is suitable for use in IP, ICC, dual RNA-FISH, iDISCO+, IEM, and FLOW. This antibody can be used to detect RFP by ELISA (sandwich or capture) for the direct binding of antigen. Biotin conjugated polyclonal anti-RFP used in a sandwich ELISA with unconjugated anti-RFP is well suited to titrate RFP in solution. The detection antibody conjugated to biotin is subsequently reacted with streptavidin conjugated HRP . Fluorochrome conjugated polyclonal anti-RFP can be used to detect RFP by immunofluorescence microscopy in cell expression systems and can detect RFP containing inserts. Significant amplification of signal is achieved using fluorochrome conjugated polyclonal anti-RFP relative to the fluorescence of RFP alone. For immunoblotting use either alkaline phosphatase or peroxidase conjugated polyclonal anti-RFP to detect RFP or RFP containing proteins on western blots. Optimal titers for applications should be determined by the researcher.
Antibody Type	Primary Antibody
Storage	Store vial at -20° C or below prior to opening. This vial contains a relatively low volume of reagent (25 µL). To minimize loss of volume dilute 1:10 by adding 225 µL of the buffer stated above directly to the vial. Recap, mix thoroughly and briefly centrifuge to collect the volume at the bottom of the vial. Use this intermediate dilution when calculating final dilutions as recommended below. Store the vial at -20°C or below after dilution. Avoid cycles of freezing and thawing.
Dry Ice Shipping	**Please note: This product requires shipment on dry ice. A dry ice surcharge will apply.**

Biorbyt Ltd.
7 Signet Court, Swann Road
Cambridge
CB5 8LA
United Kingdom
Email: info@biorbyt.com, support@biorbyt.com
Phone: +44 (0)1223 859353 | Fax: +1 (415) 651-8558

Biorbyt LLC
68 TW Alexander Drive
Research Triangle Park
Durham
NC 27713-2847
United States
Email: info@biorbyt.com, support@biorbyt.com
Phone: +1 (415) 906-5211 | Fax: +1 (415) 651-8558

Note For research use only

Expiration Date 12 months from date of receipt.

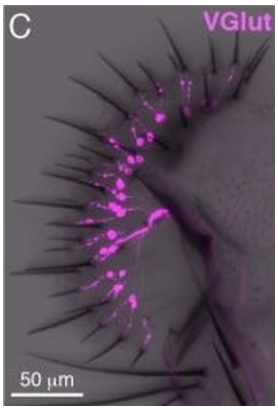

A molecular map of the fly labellum.(A) A schematic of sensillum identities in the fly labellum. (B) A summary of how GRN identities are currently viewed across the three sensillum types, with each color representing a GRN class with its most notable molecular label (if known) and its ascribed response properties. (C–H) Single labellar palps immunolabelled for VGlut-Gal4 driving UAS-tdTomato (magenta) alone (C) or in combination with LexAop-CD2::GFP (green) under the control of ChAT-LexA (D), Ppk28-LexA (E), Gr64f-LexA (F), Gr66a-LexA (G), or Ppk23-LexA (H). (I) Ppk23-LexA (green) and Gr66a-Gal4 (magenta) label partially overlapping populations. Arrows indicate sensilla where two Ppk23 GRNs exist, one of which co-expresses Gr66a. (J–K) Ppk23 subpopulations displayed by restricting Ppk23-Gal4 expression with VGlut-Gal80 (J), or Gr66a-LexA and LexAop-Gal80 (K). (L–N) IR94e-Gal4 labellum expression (magenta), co-labelled with Ppk28-LexA (L), Gr64f-LexA (M), and Ppk23-LexA (N). (O) Summary of newly defined GRN types following our mapping experiments. (P) Detailed map of each sensillum. Colors of '+' in chart indicate cell type. Grey denotes unknown identity. The VGlut + GRNs observed in I-type sensilla were sporadic and small, which is why they are not considered in the summary. Molecular mapping of characterized and uncharacterized labellar GRN types.(A) Labellum expression of Ppk23-Gal4 restricted with ChAT-Gal80. Arrow indicates an S-type sensillum with two Ppk23 + GRNs, indicating incomplete elimination of Ppk23chat expression. (B) Ppk23-Gal4 (magenta) and Ppk23-LexA (green) label nearly identical labellar GRN populations. (C–F) IR76b-Gal4 expression (magenta) in labella co-labelled with markers for different GRN populations (green): Ppk28-LexA (C), Gr64f-LexA (D), Gr66a-LexA (E), and Ppk23-LexA (F). (G) IR94e projections to the brain revealed by IR94e-Gal4 driving UAS-CsChrimson (green). Neuropil is labelled with nc82 (magenta).

Biorbyt Ltd.
7 Signet Court, Swann Road
Cambridge
CB5 8LA
United Kingdom
Email: info@biorbyt.com, support@biorbyt.com
Phone: +44 (0)1223 859353 | Fax: +1 (415) 651-8558

Biorbyt LLC
68 TW Alexander Drive
Research Triangle Park
Durham
NC 27713-2847
United States
Email: info@biorbyt.com, support@biorbyt.com
Phone: +1 (415) 906-5211 | Fax: +1 (415) 651-8558

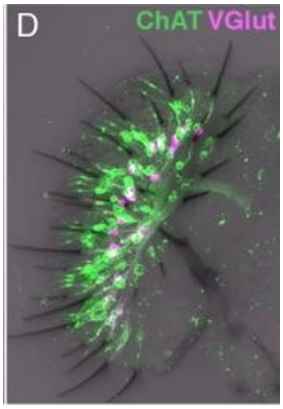

A molecular map of the fly labellum.(A) A schematic of sensillum identities in the fly labellum. (B) A summary of how GRN identities are currently viewed across the three sensillum types, with each color representing a GRN class with its most notable molecular label (if known) and its ascribed response properties. (C–H) Single labellar palps immunolabelled for VGlut-Gal4 driving UAS-tdTomato (magenta) alone (C) or in combination with LexAop-CD2::GFP (green) under the control of ChAT-LexA (D), Ppk28-LexA (E), Gr64f-LexA (F), Gr66a-LexA (G), or Ppk23-LexA (H). (I) Ppk23-LexA (green) and Gr66a-Gal4 (magenta) label partially overlapping populations. Arrows indicate sensilla where two Ppk23 GRNs exist, one of which co-expresses Gr66a. (J–K) Ppk23 subpopulations displayed by restricting Ppk23-Gal4 expression with VGlut-Gal80 (J), or Gr66a-LexA and LexAop-Gal80 (K). (L–N) IR94e-Gal4 labellum expression (magenta), co-labelled with Ppk28-LexA (L), Gr64f-LexA (M), and Ppk23-LexA (N). (O) Summary of newly defined GRN types following our mapping experiments. (P) Detailed map of each sensillum. Colors of '+' in chart indicate cell type. Grey denotes unknown identity. The VGlut + GRNs observed in I-type sensilla were sporadic and small, which is why they are not considered in the summary. Molecular mapping of characterized and uncharacterized labellar GRN types.(A) Labellum expression of Ppk23-Gal4 restricted with ChAT-Gal80. Arrow indicates an S-type sensillum with two Ppk23 + GRNs, indicating incomplete elimination of Ppk23chat expression. (B) Ppk23-Gal4 (magenta) and Ppk23-LexA (green) label nearly identical labellar GRN populations. (C–F) IR76b-Gal4 expression (magenta) in labella co-labelled with markers for different GRN populations (green): Ppk28-LexA (C), Gr64f-LexA (D), Gr66a-LexA (E), and Ppk23-LexA (F). (G) IR94e projections to the brain revealed by IR94e-Gal4 driving UAS-CsChrimson (green). Neuropil is labelled with nc82 (magenta).

Biorbyt Ltd.
7 Signet Court, Swann Road
Cambridge
CB5 8LA
United Kingdom
Email: info@biorbyt.com, support@biorbyt.com
Phone: +44 (0)1223 859353 | Fax: +1 (415) 651-8558

Biorbyt LLC
68 TW Alexander Drive
Research Triangle Park
Durham
NC 27713-2847
United States
Email: info@biorbyt.com, support@biorbyt.com
Phone: +1 (415) 906-5211 | Fax: +1 (415) 651-8558

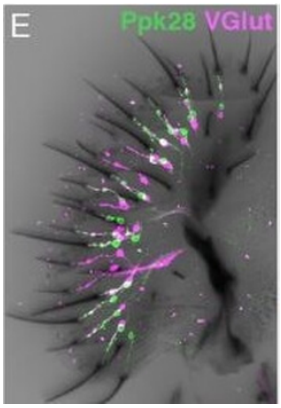

A molecular map of the fly labellum.(A) A schematic of sensillum identities in the fly labellum. (B) A summary of how GRN identities are currently viewed across the three sensillum types, with each color representing a GRN class with its most notable molecular label (if known) and its ascribed response properties. (C–H) Single labellar palps immunolabelled for VGlut-Gal4 driving UAS-tdTomato (magenta) alone (C) or in combination with LexAop-CD2::GFP (green) under the control of ChAT-LexA (D), Ppk28-LexA (E), Gr64f-LexA (F), Gr66a-LexA (G), or Ppk23-LexA (H). (I) Ppk23-LexA (green) and Gr66a-Gal4 (magenta) label partially overlapping populations. Arrows indicate sensilla where two Ppk23 GRNs exist, one of which co-expresses Gr66a. (J–K) Ppk23 subpopulations displayed by restricting Ppk23-Gal4 expression with VGlut-Gal80 (J), or Gr66a-LexA and LexAop-Gal80 (K). (L–N) IR94e-Gal4 labellum expression (magenta), co-labelled with Ppk28-LexA (L), Gr64f-LexA (M), and Ppk23-LexA (N). (O) Summary of newly defined GRN types following our mapping experiments. (P) Detailed map of each sensillum. Colors of '+' in chart indicate cell type. Grey denotes unknown identity. The VGlut + GRNs observed in I-type sensilla were sporadic and small, which is why they are not considered in the summary. Molecular mapping of characterized and uncharacterized labellar GRN types.(A) Labellum expression of Ppk23-Gal4 restricted with ChAT-Gal80. Arrow indicates an S-type sensillum with two Ppk23 + GRNs, indicating incomplete elimination of Ppk23chat expression. (B) Ppk23-Gal4 (magenta) and Ppk23-LexA (green) label nearly identical labellar GRN populations. (C–F) IR76b-Gal4 expression (magenta) in labella co-labelled with markers for different GRN populations (green): Ppk28-LexA (C), Gr64f-LexA (D), Gr66a-LexA (E), and Ppk23-LexA (F). (G) IR94e projections to the brain revealed by IR94e-Gal4 driving UAS-CsChrimson (green). Neuropil is labelled with nc82 (magenta).

Biorbyt Ltd.
7 Signet Court, Swann Road
Cambridge
CB5 8LA
United Kingdom
Email: info@biorbyt.com, support@biorbyt.com
Phone: +44 (0)1223 859353 | Fax: +1 (415) 651-8558

Biorbyt LLC
68 TW Alexander Drive
Research Triangle Park
Durham
NC 27713-2847
United States
Email: info@biorbyt.com, support@biorbyt.com
Phone: +1 (415) 906-5211 | Fax: +1 (415) 651-8558

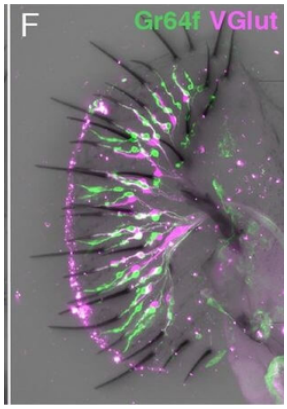

A molecular map of the fly labellum.(A) A schematic of sensillum identities in the fly labellum. (B) A summary of how GRN identities are currently viewed across the three sensillum types, with each color representing a GRN class with its most notable molecular label (if known) and its ascribed response properties. (C–H) Single labellar palps immunolabelled for VGlut-Gal4 driving UAS-tdTomato (magenta) alone (C) or in combination with LexAop-CD2::GFP (green) under the control of ChAT-LexA (D), Ppk28-LexA (E), Gr64f-LexA (F), Gr66a-LexA (G), or Ppk23-LexA (H). (I) Ppk23-LexA (green) and Gr66a-Gal4 (magenta) label partially overlapping populations. Arrows indicate sensilla where two Ppk23 GRNs exist, one of which co-expresses Gr66a. (J–K) Ppk23 subpopulations displayed by restricting Ppk23-Gal4 expression with VGlut-Gal80 (J), or Gr66a-LexA and LexAop-Gal80 (K). (L–N) IR94e-Gal4 labellum expression (magenta), co-labelled with Ppk28-LexA (L), Gr64f-LexA (M), and Ppk23-LexA (N). (O) Summary of newly defined GRN types following our mapping experiments. (P) Detailed map of each sensillum. Colors of '+' in chart indicate cell type. Grey denotes unknown identity. The VGlut + GRNs observed in I-type sensilla were sporadic and small, which is why they are not considered in the summary. Molecular mapping of characterized and uncharacterized labellar GRN types.(A) Labellum expression of Ppk23-Gal4 restricted with ChAT-Gal80. Arrow indicates an S-type sensillum with two Ppk23 + GRNs, indicating incomplete elimination of Ppk23chat expression. (B) Ppk23-Gal4 (magenta) and Ppk23-LexA (green) label nearly identical labellar GRN populations. (C–F) IR76b-Gal4 expression (magenta) in labella co-labelled with markers for different GRN populations (green): Ppk28-LexA (C), Gr64f-LexA (D), Gr66a-LexA (E), and Ppk23-LexA (F). (G) IR94e projections to the brain revealed by IR94e-Gal4 driving UAS-CsChrimson (green). Neuropil is labelled with nc82 (magenta).

Biorbyt Ltd.
7 Signet Court, Swann Road
Cambridge
CB5 8LA
United Kingdom
Email: info@biorbyt.com, support@biorbyt.com
Phone: +44 (0)1223 859353 | Fax: +1 (415) 651-8558

Biorbyt LLC
68 TW Alexander Drive
Research Triangle Park
Durham
NC 27713-2847
United States
Email: info@biorbyt.com, support@biorbyt.com
Phone: +1 (415) 906-5211 | Fax: +1 (415) 651-8558

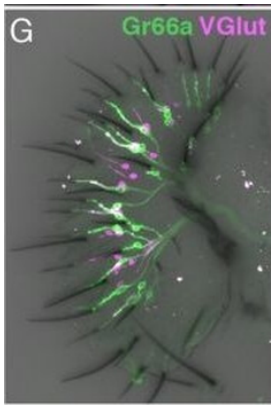

A molecular map of the fly labellum.(A) A schematic of sensillum identities in the fly labellum. (B) A summary of how GRN identities are currently viewed across the three sensillum types, with each color representing a GRN class with its most notable molecular label (if known) and its ascribed response properties. (C–H) Single labellar palps immunolabelled for VGlut-Gal4 driving UAS-tdTomato (magenta) alone (C) or in combination with LexAop-CD2::GFP (green) under the control of ChAT-LexA (D), Ppk28-LexA (E), Gr64f-LexA (F), Gr66a-LexA (G), or Ppk23-LexA (H). (I) Ppk23-LexA (green) and Gr66a-Gal4 (magenta) label partially overlapping populations. Arrows indicate sensilla where two Ppk23 GRNs exist, one of which co-expresses Gr66a. (J–K) Ppk23 subpopulations displayed by restricting Ppk23-Gal4 expression with VGlut-Gal80 (J), or Gr66a-LexA and LexAop-Gal80 (K). (L–N) IR94e-Gal4 labellum expression (magenta), co-labelled with Ppk28-LexA (L), Gr64f-LexA (M), and Ppk23-LexA (N). (O) Summary of newly defined GRN types following our mapping experiments. (P) Detailed map of each sensillum. Colors of '+' in chart indicate cell type. Grey denotes unknown identity. The VGlut + GRNs observed in I-type sensilla were sporadic and small, which is why they are not considered in the summary. Molecular mapping of characterized and uncharacterized labellar GRN types.(A) Labellum expression of Ppk23-Gal4 restricted with ChAT-Gal80. Arrow indicates an S-type sensillum with two Ppk23 + GRNs, indicating incomplete elimination of Ppk23chat expression. (B) Ppk23-Gal4 (magenta) and Ppk23-LexA (green) label nearly identical labellar GRN populations. (C–F) IR76b-Gal4 expression (magenta) in labella co-labelled with markers for different GRN populations (green): Ppk28-LexA (C), Gr64f-LexA (D), Gr66a-LexA (E), and Ppk23-LexA (F). (G) IR94e projections to the brain revealed by IR94e-Gal4 driving UAS-CsChrimson (green). Neuropil is labelled with nc82 (magenta).

Biorbyt Ltd.
7 Signet Court, Swann Road
Cambridge
CB5 8LA
United Kingdom
Email: info@biorbyt.com, support@biorbyt.com
Phone: +44 (0)1223 859353 | Fax: +1 (415) 651-8558

Biorbyt LLC
68 TW Alexander Drive
Research Triangle Park
Durham
NC 27713-2847
United States
Email: info@biorbyt.com, support@biorbyt.com
Phone: +1 (415) 906-5211 | Fax: +1 (415) 651-8558

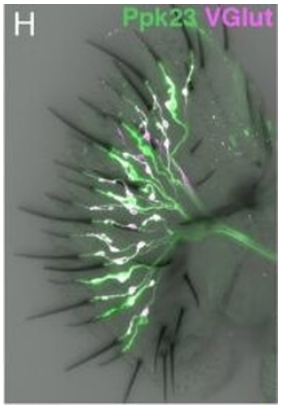

A molecular map of the fly labellum.(A) A schematic of sensillum identities in the fly labellum. (B) A summary of how GRN identities are currently viewed across the three sensillum types, with each color representing a GRN class with its most notable molecular label (if known) and its ascribed response properties. (C–H) Single labellar palps immunolabelled for VGlut-Gal4 driving UAS-tdTomato (magenta) alone (C) or in combination with LexAop-CD2::GFP (green) under the control of ChAT-LexA (D), Ppk28-LexA (E), Gr64f-LexA (F), Gr66a-LexA (G), or Ppk23-LexA (H). (I) Ppk23-LexA (green) and Gr66a-Gal4 (magenta) label partially overlapping populations. Arrows indicate sensilla where two Ppk23 GRNs exist, one of which co-expresses Gr66a. (J–K) Ppk23 subpopulations displayed by restricting Ppk23-Gal4 expression with VGlut-Gal80 (J), or Gr66a-LexA and LexAop-Gal80 (K). (L–N) IR94e-Gal4 labellum expression (magenta), co-labelled with Ppk28-LexA (L), Gr64f-LexA (M), and Ppk23-LexA (N). (O) Summary of newly defined GRN types following our mapping experiments. (P) Detailed map of each sensillum. Colors of '+' in chart indicate cell type. Grey denotes unknown identity. The VGlut + GRNs observed in I-type sensilla were sporadic and small, which is why they are not considered in the summary. Molecular mapping of characterized and uncharacterized labellar GRN types.(A) Labellum expression of Ppk23-Gal4 restricted with ChAT-Gal80. Arrow indicates an S-type sensillum with two Ppk23 + GRNs, indicating incomplete elimination of Ppk23chat expression. (B) Ppk23-Gal4 (magenta) and Ppk23-LexA (green) label nearly identical labellar GRN populations. (C–F) IR76b-Gal4 expression (magenta) in labella co-labelled with markers for different GRN populations (green): Ppk28-LexA (C), Gr64f-LexA (D), Gr66a-LexA (E), and Ppk23-LexA (F). (G) IR94e projections to the brain revealed by IR94e-Gal4 driving UAS-CsChrimson (green). Neuropil is labelled with nc82 (magenta).

Biorbyt Ltd.
7 Signet Court, Swann Road
Cambridge
CB5 8LA
United Kingdom
Email: info@biorbyt.com, support@biorbyt.com
Phone: +44 (0)1223 859353 | Fax: +1 (415) 651-8558

Biorbyt LLC
68 TW Alexander Drive
Research Triangle Park
Durham
NC 27713-2847
United States
Email: info@biorbyt.com, support@biorbyt.com
Phone: +1 (415) 906-5211 | Fax: +1 (415) 651-8558

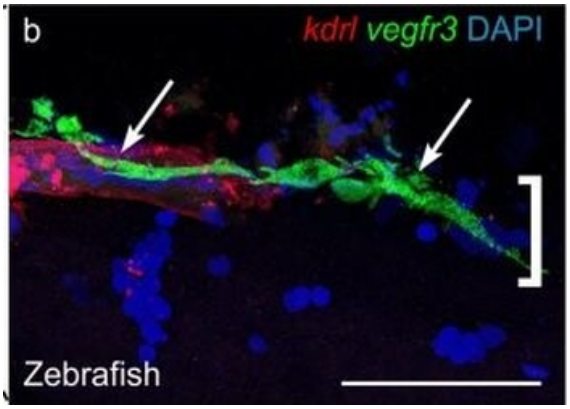

Cells with BLEC molecular markers are present within the mouse leptomeninges. a Coronal brain section of adult zebrafish brain indicating the imaging area in the dorsal optic tectum (TeO). b A 14 month old Tg(kdr-l:mCherry); Tg(flt4:mCitrine) double transgenic zebrafish has cells in the meninges (white bracket) that express flt4/vegfr3 (α-GFP, green) near kdr-l positive (α-RFP, red) blood vessels. DAPI (blue) labels the nuclei. Scale = 50 µm. c Coronal mouse brain section showing the imaging areas of the meninges. d As revealed by IHC, 17-week-old mouse brains express VEGFR3 (green) in the meninges (white bracket). Tie2-GFP;NG2-DsRed double reporter mice were used to distinguish arteries and veins. NG2 (red) labels pericytes and smooth muscle cells, Tie2 (magenta) labels vascular endothelial cells, and Hoechst (blue) stains nuclei. The image is rotated with the parenchyma at the bottom for ease of comparison with panel b. Scale = 50 µm. e-e"' As revealed by IHC, cells of the meninges co-express MRC1 (e, yellow), LYVE1 (e', white), and VEGFR3 (e", green). Red arrows highlight cells expressing these three markers. The images are rotated with the parenchyma at the bottom. scale = 30 µm. f, g Quantification of the relative numbers of single and double-labelled cells in 2-month old mouse meninges. VEGFR3 and LYVE1 cell counts were from n = 2 brains, 3 coronal sections (10 area images)/brain. MRC1 and LYVE1 cell counts were from n = 3 brains, 3 coronal sections (4 area images)/brain. The mean values for each set are depicted.

Biorbyt Ltd.
7 Signet Court, Swann Road
Cambridge
CB5 8LA
United Kingdom
Email: info@biorbyt.com, support@biorbyt.com
Phone: +44 (0)1223 859353 | Fax: +1 (415) 651-8558

Biorbyt LLC
68 TW Alexander Drive
Research Triangle Park
Durham
NC 27713-2847
United States
Email: info@biorbyt.com, support@biorbyt.com
Phone: +1 (415) 906-5211 | Fax: +1 (415) 651-8558

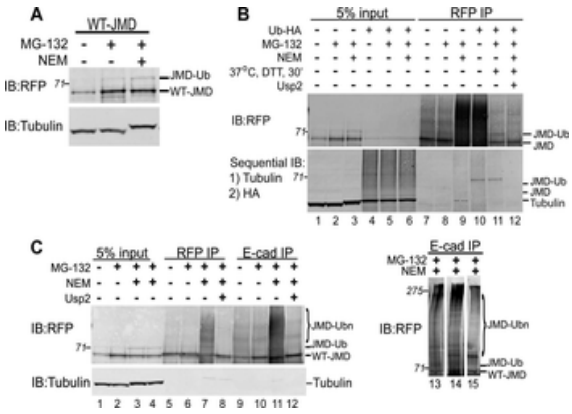

E-cadherin JMD is Ubiquitinated.(A) Lysates of WT-JMD stable cell lines under normal conditions, upon proteasome inhibition (MG-132), or inhibition of deubiquitinating enzymes (NEM). Immunoblot (IB) for RFP shows a slower migrating band (JMD-Ub) in the presence of MG-132 and NEM. (B) In a separate experiment MDCK cells stably expressing WT-JMD were transiently transfected with Ub-HA where indicated. Cells were extracted and RFP immunoprecipitations were preformed under normal conditions, upon proteasome inhibition, NEM treatment (to inhibit de-ubiquitinating enzymes), addition of the deubiquitinating enzyme Usp2, or mock transfections. DTT was added to the immunoprecipitates after the final was of Protein A beads but prior to the addition of Usp2, where indicated, to neutralize residual NEM. Immunoblots (IB) were performed for RFP using a rabbit polyclonal antibody, followed by a sequential immunoblotting with antibodies specific for: 1) tubulin; and 2) HA. The slowest migrating band (marked as JMD-Ub) that appears in the presence of NEM is positive for RFP and HA (lanes 10 and 11). HC denotes IgG heavy chain. Number(s) on the side of the gels are the apparent molecular weights of protein standards (× 10∧3). (C) Extracts from MDCK cells stably expressing WT-JMD were immunoprecipitated (IP) for RFP and E-cadherin under normal conditions, upon proteasome inhibition, NEM treatment (to inhibit de-ubiquitinating enzymes), or addition of the de-ubiquitinating enzyme Usp2. DTT was added to the immunoprecipitates after the final wash of Protein A beads but prior to the addition of Usp2, where indicated, to neutralize residual NEM. A slow migrating band (lane 15) and protein smear (lanes 11, 13, and 14) appear in E-cadherin immunoprecipitates in the presence of NEM, and collapse upon incubation with Usp2 (similar to RFP immunoprecipitates). RFP immunoblots in lanes 11, 13, 14 & 15 show that the slower migrating band does migrates at different molecular weights indicating variable levels of JMD ubiquitination. Number(s) on the side of the blots are the apparent molecular weights of protein standards (× 10∧3). Data are representative of 3 different experiments.

Biorbyt Ltd.
7 Signet Court, Swann Road
Cambridge
CB5 8LA
United Kingdom
Email: info@biorbyt.com, support@biorbyt.com
Phone: +44 (0)1223 859353 | Fax: +1 (415) 651-8558

Biorbyt LLC
68 TW Alexander Drive
Research Triangle Park
Durham
NC 27713-2847
United States
Email: info@biorbyt.com, support@biorbyt.com
Phone: +1 (415) 906-5211 | Fax: +1 (415) 651-8558

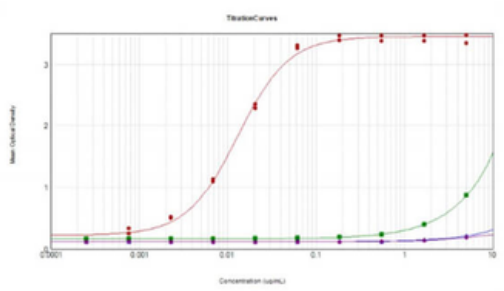

ELISA Results of Polyclonal Rabbit Anti-RFP Antibody tested against purified RFP protein. Each well was coated in duplicate with 1.0 µg of RFP (p/n orb345960) [red], Human IgG (p/n orb346219) [green], Mouse IgG (p/n orb2652749) [blue], Rat IgG (p/n orb2652744) [purple]. The starting dilution of antibody was 5 µg/ml and the X-axis represents the Log10 of a 3-fold dilution. This titration is a 4-parameter curve fit where the IC50 is defined as the titer of the antibody. Assay performed using 1% Fish Gel in PBS Blocking Buffer, Goat Anti-Rabbit IgG HRP conjugated (p/n orb347654) and TMB substrate (p/n orb348651). Results show RFP titer > 75000, Human, Mouse, Rat IgG titers 100.

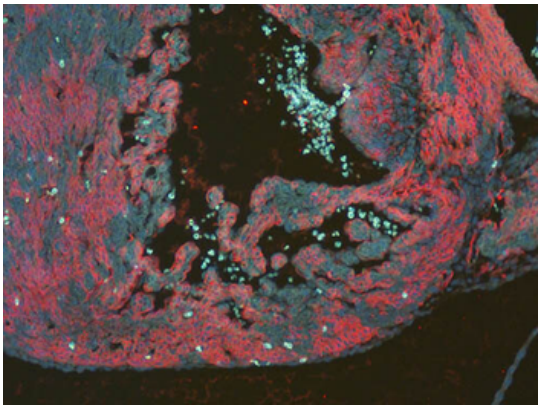

Immunofluorescence Microscopy of Rabbit Anti-RFP antibody. Tissue: (10X) Mouse E14.5 embryo heart tissue. Fixation: 4% PFA. Antigen retrieval: Heat. Primary antibody: Anti-RFP antibody at 1:50 for 1 h at RT. Secondary antibody: Fluorescein rabbit secondary antibody at 1:250 for 1 hr at RT. Staining: cardiac cells are RFP positive in red in tomato transgenic mice.

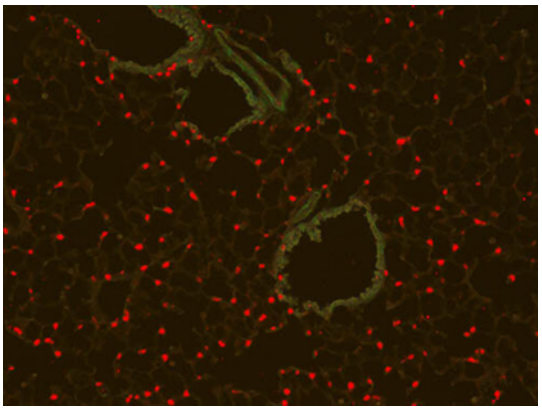

Immunofluorescence Microscopy of Rabbit Anti-RFP antibody. Tissue: (10X) Mouse lung tissue. Fixation: 4% PFA. Antigen retrieval: Heat. Primary antibody: Anti-RFP antibody at 1:50 for 1 h at RT. Secondary antibody: Fluorescein rabbit secondary antibody at 1:250 for 1 hr at RT. Staining: SPC + cells are RFP positive in red.

Biorbyt Ltd.
7 Signet Court, Swann Road
Cambridge
CB5 8LA
United Kingdom
Email: info@biorbyt.com, support@biorbyt.com
Phone: +44 (0)1223 859353 | Fax: +1 (415) 651-8558

Biorbyt LLC
68 TW Alexander Drive
Research Triangle Park
Durham
NC 27713-2847
United States
Email: info@biorbyt.com, support@biorbyt.com
Phone: +1 (415) 906-5211 | Fax: +1 (415) 651-8558

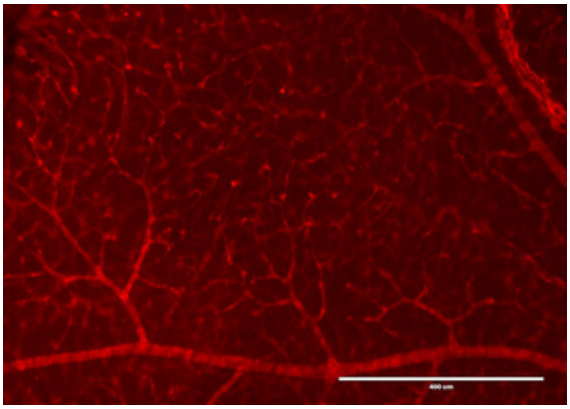

Immunofluorescence Microscopy of Rabbit Anti-RFP antibody. Tissue: DsRed transgenic mouse retina. Fixation: 4% PFA. Blocking: 3% BSA, 0.3% Triton Primary antibody: RFP antibody at 1:100 for 12 h at 4°C. Secondary antibody: Alexa488 secondary antibody at 1:10000 for 4 hours at RT. Localization: RFP is nuclear and occasionally cytoplasmic. Staining: labeled in red.

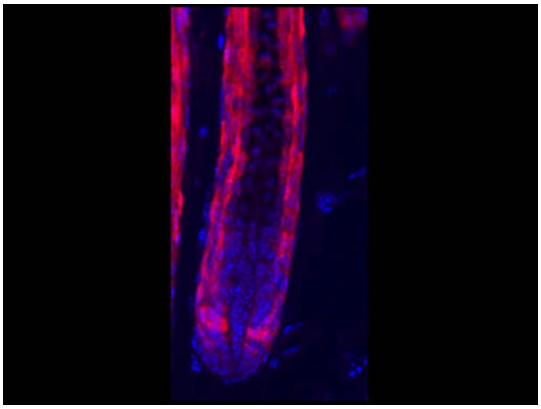

Immunofluorescence Microscopy of Rabbit Anti-RFP antibody. Tissue: HopERCre/+ ; R26Tom/+ mice. Fixation: 0.5% PFA. Antigen retrieval: Tamoxifen. Primary antibody: RFP antibody at 10 µg/ml for 1 h at RT. Secondary antibody: Fluorescein rabbit secondary antibody at 1:10000 for 45 min at RT. Localization: RFP is nuclear and occasionally cytoplasmic. Staining: Hop-derived cells in the hair follicle, labeled in red.

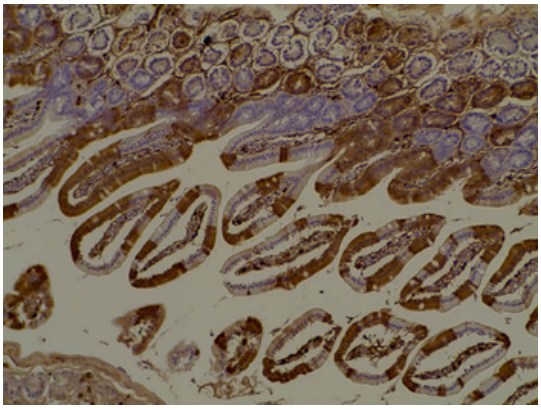

Immunohistochemistry of Anti-RFP Antibody. Tissue: Mouse gut tissue in tomato transgenic mice. Fixation: formalin fixed paraffin embedded. Antigen retrieval: heat 5 min at high temp in 1X rodent decloaker. Primary antibody: RFP antibody at 1:200 for 1 h 30 min at RT. Secondary Antibody: HRP anti-rabbit (p/n orb347654).

Biorbyt Ltd.
7 Signet Court, Swann Road
Cambridge
CB5 8LA
United Kingdom
Email: info@biorbyt.com, support@biorbyt.com
Phone: +44 (0)1223 859353 | Fax: +1 (415) 651-8558

Biorbyt LLC
68 TW Alexander Drive
Research Triangle Park
Durham
NC 27713-2847
United States
Email: info@biorbyt.com, support@biorbyt.com
Phone: +1 (415) 906-5211 | Fax: +1 (415) 651-8558

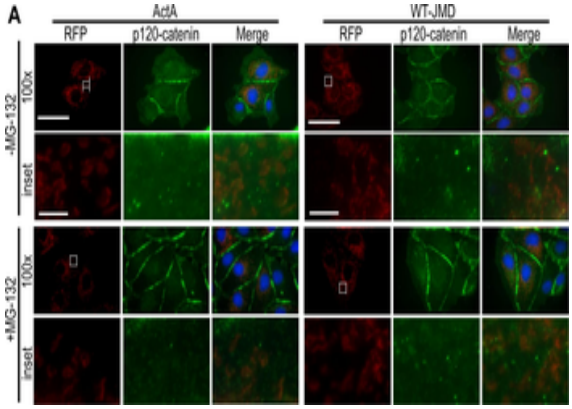

Localization and binding of WT-JMD and p120-catenin.(A) Immunofluorescence of MDCK cells transiently expressing ActA or WT-JMD. Images for RFP (red), p120-catenin (green) and merged are shown separately (100×). Boxed areas are shown as higher magnifications below (RFP-, p120- and merge-inset). All images were from the same experiment and processed identically between cell lines. Scale bar is 25 µm in 100× images, and 5 µm in insets. (B) Lysates and RFP immunoprecipitates (IP) of ActA and WT-JMD stable cell lines under normal conditions, upon proteasome inhibition, or NEM treatment (to inhibit de-ubiquitinating enzymes). Immunoblots (IB) for RFP show: a slower migrating band (upper band-JMD-Ub) that appears only in WT-JMD cells in the presence of MG-132 and NEM; the band identified as ActA/HC comprises a co-migrating ActA and the IgG heavy chain (HC). Number(s) on the side of the gels are the apparent molecular weights of protein standards (× 10∧3). (C) Quantification of RFP intensities normalized to tubulin in WT-JMD stables cell lines. Data averaged from 3 independent experiments (+/− s.e.m.), and 2 independently cloned stable cell lines; *p ≤ 0.05, **p ≤ 0.01.

Biorbyt Ltd.
7 Signet Court, Swann Road
Cambridge
CB5 8LA
United Kingdom
Email: info@biorbyt.com, support@biorbyt.com
Phone: +44 (0)1223 859353 | Fax: +1 (415) 651-8558

Biorbyt LLC
68 TW Alexander Drive
Research Triangle Park
Durham
NC 27713-2847
United States
Email: info@biorbyt.com, support@biorbyt.com
Phone: +1 (415) 906-5211 | Fax: +1 (415) 651-8558

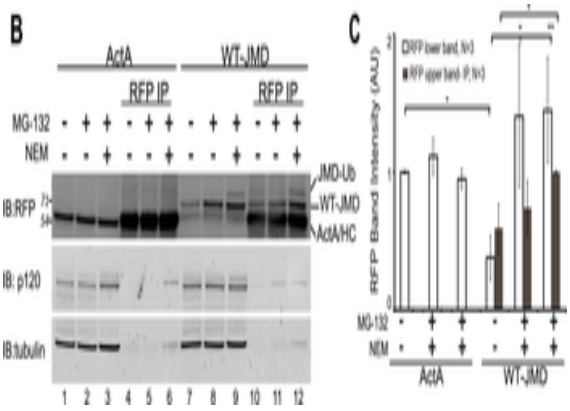

Localization and binding of WT-JMD and p120-catenin.(A) Immunofluorescence of MDCK cells transiently expressing ActA or WT-JMD. Images for RFP (red), p120-catenin (green) and merged are shown separately (100×). Boxed areas are shown as higher magnifications below (RFP-, p120- and merge-inset). All images were from the same experiment and processed identically between cell lines. Scale bar is 25 µm in 100× images, and 5 µm in insets. (B) Lysates and RFP immunoprecipitates (IP) of ActA and WT-JMD stable cell lines under normal conditions, upon proteasome inhibition, or NEM treatment (to inhibit de-ubiquitinating enzymes). Immunoblots (IB) for RFP show: a slower migrating band (upper band-JMD-Ub) that appears only in WT-JMD cells in the presence of MG-132 and NEM; the band identified as ActA/HC comprises a co-migrating ActA and the IgG heavy chain (HC). Number(s) on the side of the gels are the apparent molecular weights of protein standards (× 10∧3). (C) Quantification of RFP intensities normalized to tubulin in WT-JMD stables cell lines. Data averaged from 3 independent experiments (+/− s.e.m.), and 2 independently cloned stable cell lines; *p ≤ 0.05, **p ≤ 0.01.

Biorbyt Ltd.
7 Signet Court, Swann Road
Cambridge
CB5 8LA
United Kingdom
Email: info@biorbyt.com, support@biorbyt.com
Phone: +44 (0)1223 859353 | Fax: +1 (415) 651-8558

Biorbyt LLC
68 TW Alexander Drive
Research Triangle Park
Durham
NC 27713-2847
United States
Email: info@biorbyt.com, support@biorbyt.com
Phone: +1 (415) 906-5211 | Fax: +1 (415) 651-8558

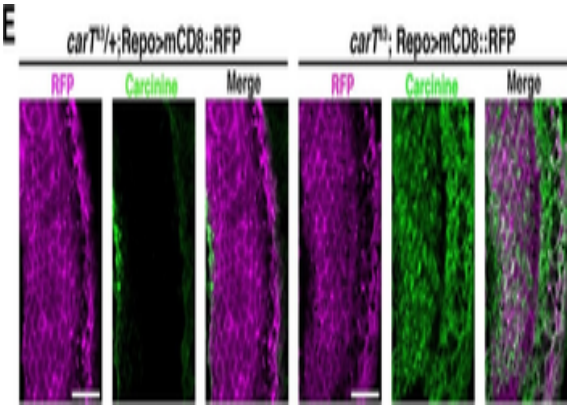

Loss of CarT in photoreceptors increases laminal carcinine.(A) Confocal sections of photoreceptor axonal endings within the lamina stained for the synapse marker Bruchpilot (Brp) and the glia-specific Ebony. (B) Micrographs of cryo-sections from control (OreR) and flies expressing the UAS-Myc-CarT transgene driven by longGMR-Gal4 in the carT43 background. Retina (R), lamina (L), and medulla (M) neuropiles are stained for DNA (magenta) and Myc-tagged CarT (green). Arrow points to Myc staining in photoreceptor axonal endings and arrowhead to distal retina. (C, D) Micrographs of cryo-sections from control (OreR) and mutant flies affecting the histamine–carcinine cycle: carT43, carT43;GMR-Gal4/UAS-Myc-CarT, ebony1, tan1, and HdcMB07212 stained for histamine (C) or carcinine (D). Arrow and arrowhead in D point to carcinine accumulations in the lamina and medulla, respectively. (E) Micrographs from control (carT43/+) or carT43 flies expressing a UAS-mCD8::RFP transgene driven by repo-Gal4 and stained for carcinine. (F) Micrographs showing tdTomato fluorescence of the in-frame tdTomato-CarT allele compared with wild type control. DNA staining is shown in green. Arrowheads point to tdTomato signal at R7 and R8 photoreceptor terminals within the medulla. (G) Confocal section of laminal region of a tdTomato-CarT fly stained for glia-specific Ebony. (H) Confocal sections of flies heterozygous for tdTomato-CarT (red) and photoreceptor-specific 3xPax3-eGFP (blue) stained for Brp (green). Sections are parallel to and across photoreceptor axons, respectively. Scale bars are 20 μm in A, E, G and H and 50 μm in B–D and F.

Biorbyt Ltd.
7 Signet Court, Swann Road
Cambridge
CB5 8LA
United Kingdom
Email: info@biorbyt.com, support@biorbyt.com
Phone: +44 (0)1223 859353 | Fax: +1 (415) 651-8558

Biorbyt LLC
68 TW Alexander Drive
Research Triangle Park
Durham
NC 27713-2847
United States
Email: info@biorbyt.com, support@biorbyt.com
Phone: +1 (415) 906-5211 | Fax: +1 (415) 651-8558

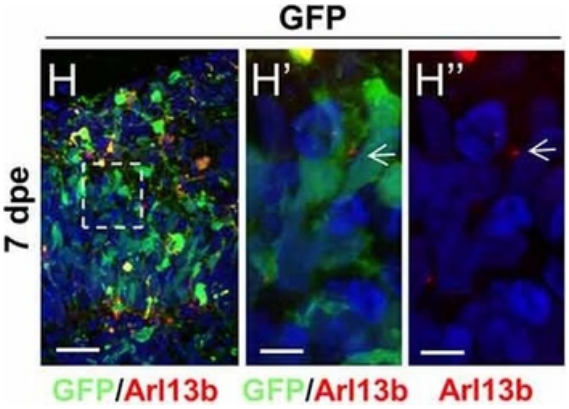

Mob2 knockdown alters neuronal cell distribution and nucleus-cilia coupling. Coronal micrograph sections of E16 mouse cerebral cortices electroporated at E13 with EGFP/empty vector control (A) or miRNAs targeting Mob2(B). (C) Quantification of the distribution of EGFP-expressing (EGFP+) cells transfected with EGFP/empty vector alone or miRNAs targeting Mob2 3 days after electroporation (mean ± SEM). The cortex was subdivided into five equal width bins approximately corresponding to VZ (bin 1), SVZ (bin 2), IZ (bin 3) and CP (bins 4 and 5). CP, cortical plate; IZ, intermediate zone; SVZ, subventricular zone; VZ, ventricular zone; dpe, days post electroporation. At least three embryos were analyzed for each condition. n, total number of GFP + cells counted per condition. (D, E) Representative images of migrating neurons in E16 cortices (3 dpe) electroporated with EGFP/control or miRNA targeting Mob2 (green) and Arl13b-tagRFP (red) located within bin 5 (CP2). Arrow heads indicate the cell bodies and arrows indicate the cilia labeled by Arl13b-tagRFP. Asterisks show the position of three cilia within a neuron. (F) Quantification of the distance between the cilia and nucleus (micrometers) in neurons. Each dot represents a neuron and red lines indicate mean ± SEM. (G) Quantification of the number of cilia in each neuron. (H, I) Micrographs sections of day 51 human cerebral organoids electroporated at day 44 with EGFP/empty vector control or miRNA targeting MOB2 (green) and Arl13b-tagRFP (red). White arrows indicate the cilia labeled by Arl13b-tagRFP. (J) Quantification of the percentage of cells with more than one cilium of organoids transfected with EGFP/empty vector control (GFP) or miRNAs targeting Mob2. Data taken from at least three ventricular structures. (C, F, G) Mann-Whitney U test, (J) Exact binomial test; *p 0.05, ***p 0.001. Scale bar represents (A, B) 100 µm, (D, E) 10 µm, (H, I) 25 µm and (H', H″, I', I″) 5 µm.

Biorbyt Ltd.
7 Signet Court, Swann Road
Cambridge
CB5 8LA
United Kingdom
Email: info@biorbyt.com, support@biorbyt.com
Phone: +44 (0)1223 859353 | Fax: +1 (415) 651-8558

Biorbyt LLC
68 TW Alexander Drive
Research Triangle Park
Durham
NC 27713-2847
United States
Email: info@biorbyt.com, support@biorbyt.com
Phone: +1 (415) 906-5211 | Fax: +1 (415) 651-8558

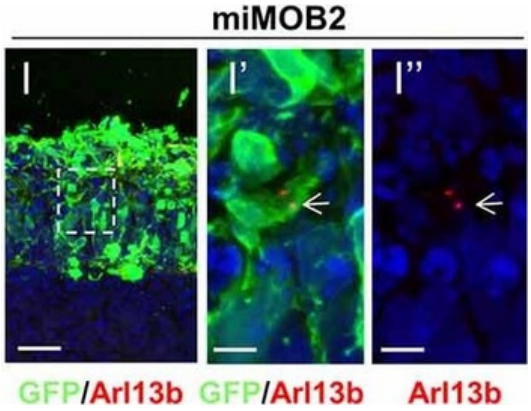

Mob2 knockdown alters neuronal cell distribution and nucleus-cilia coupling. Coronal micrograph sections of E16 mouse cerebral cortices electroporated at E13 with EGFP/empty vector control (A) or miRNAs targeting Mob2(B). (C) Quantification of the distribution of EGFP-expressing (EGFP+) cells transfected with EGFP/empty vector alone or miRNAs targeting Mob2 3 days after electroporation (mean ± SEM). The cortex was subdivided into five equal width bins approximately corresponding to VZ (bin 1), SVZ (bin 2), IZ (bin 3) and CP (bins 4 and 5). CP, cortical plate; IZ, intermediate zone; SVZ, subventricular zone; VZ, ventricular zone; dpe, days post electroporation. At least three embryos were analyzed for each condition. n, total number of GFP + cells counted per condition. (D, E) Representative images of migrating neurons in E16 cortices (3 dpe) electroporated with EGFP/control or miRNA targeting Mob2 (green) and Arl13b-tagRFP (red) located within bin 5 (CP2). Arrow heads indicate the cell bodies and arrows indicate the cilia labeled by Arl13b-tagRFP. Asterisks show the position of three cilia within a neuron. (F) Quantification of the distance between the cilia and nucleus (micrometers) in neurons. Each dot represents a neuron and red lines indicate mean ± SEM. (G) Quantification of the number of cilia in each neuron. (H, I) Micrographs sections of day 51 human cerebral organoids electroporated at day 44 with EGFP/empty vector control or miRNA targeting MOB2 (green) and Arl13b-tagRFP (red). White arrows indicate the cilia labeled by Arl13b-tagRFP. (J) Quantification of the percentage of cells with more than one cilium of organoids transfected with EGFP/empty vector control (GFP) or miRNAs targeting Mob2. Data taken from at least three ventricular structures. (C, F, G) Mann-Whitney U test, (J) Exact binomial test; *p 0.05, ***p 0.001. Scale bar represents (A, B) 100 µm, (D, E) 10 µm, (H, I) 25 µm and (H', H″, I', I″) 5 µm.

Biorbyt Ltd.
7 Signet Court, Swann Road
Cambridge
CB5 8LA
United Kingdom
Email: info@biorbyt.com, support@biorbyt.com
Phone: +44 (0)1223 859353 | Fax: +1 (415) 651-8558

Biorbyt LLC
68 TW Alexander Drive
Research Triangle Park
Durham
NC 27713-2847
United States
Email: info@biorbyt.com, support@biorbyt.com
Phone: +1 (415) 906-5211 | Fax: +1 (415) 651-8558

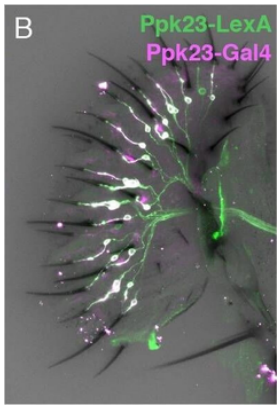

Molecular mapping of characterized and uncharacterized labellar GRN types.(A) Labellum expression of Ppk23-Gal4 restricted with ChAT-Gal80. Arrow indicates an S-type sensillum with two Ppk23 +GRNs, indicating incomplete elimination of Ppk23chat expression. (B) Ppk23-Gal4 (magenta) and Ppk23-LexA (green) label nearly identical labellar GRN populations. (C–F) IR76b-Gal4 expression (magenta) in labella co-labelled with markers for different GRN populations (green): Ppk28-LexA (C), Gr64f-LexA (D), Gr66a-LexA (E), and Ppk23-LexA (F). (G) IR94e projections to the brain revealed by IR94e-Gal4 driving UAS-CsChrimson (green). Neuropil is labelled with nc82 (magenta).

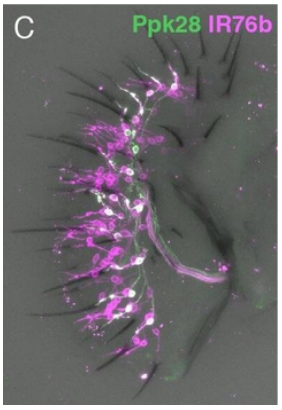

Molecular mapping of characterized and uncharacterized labellar GRN types.(A) Labellum expression of Ppk23-Gal4 restricted with ChAT-Gal80. Arrow indicates an S-type sensillum with two Ppk23 +GRNs, indicating incomplete elimination of Ppk23chat expression. (B) Ppk23-Gal4 (magenta) and Ppk23-LexA (green) label nearly identical labellar GRN populations. (C–F) IR76b-Gal4 expression (magenta) in labella co-labelled with markers for different GRN populations (green): Ppk28-LexA (C), Gr64f-LexA (D), Gr66a-LexA (E), and Ppk23-LexA (F). (G) IR94e projections to the brain revealed by IR94e-Gal4 driving UAS-CsChrimson (green). Neuropil is labelled with nc82 (magenta).

Biorbyt Ltd.
7 Signet Court, Swann Road
Cambridge
CB5 8LA
United Kingdom
Email: info@biorbyt.com, support@biorbyt.com
Phone: +44 (0)1223 859353 | Fax: +1 (415) 651-8558

Biorbyt LLC
68 TW Alexander Drive
Research Triangle Park
Durham
NC 27713-2847
United States
Email: info@biorbyt.com, support@biorbyt.com
Phone: +1 (415) 906-5211 | Fax: +1 (415) 651-8558

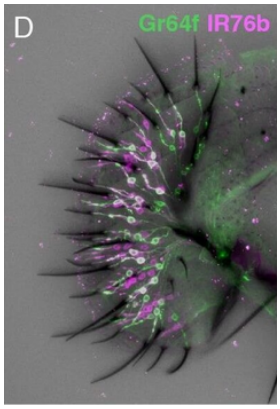

Molecular mapping of characterized and uncharacterized labellar GRN types.(A) Labellum expression of Ppk23-Gal4 restricted with ChAT-Gal80. Arrow indicates an S-type sensillum with two Ppk23 +GRNs, indicating incomplete elimination of Ppk23chat expression. (B) Ppk23-Gal4 (magenta) and Ppk23-LexA (green) label nearly identical labellar GRN populations. (C–F) IR76b-Gal4 expression (magenta) in labella co-labelled with markers for different GRN populations (green): Ppk28-LexA (C), Gr64f-LexA (D), Gr66a-LexA (E), and Ppk23-LexA (F). (G) IR94e projections to the brain revealed by IR94e-Gal4 driving UAS-CsChrimson (green). Neuropil is labelled with nc82 (magenta).

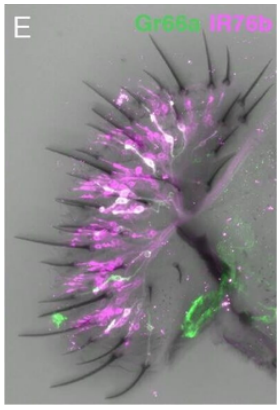

Molecular mapping of characterized and uncharacterized labellar GRN types.(A) Labellum expression of Ppk23-Gal4 restricted with ChAT-Gal80. Arrow indicates an S-type sensillum with two Ppk23 +GRNs, indicating incomplete elimination of Ppk23chat expression. (B) Ppk23-Gal4 (magenta) and Ppk23-LexA (green) label nearly identical labellar GRN populations. (C–F) IR76b-Gal4 expression (magenta) in labella co-labelled with markers for different GRN populations (green): Ppk28-LexA (C), Gr64f-LexA (D), Gr66a-LexA (E), and Ppk23-LexA (F). (G) IR94e projections to the brain revealed by IR94e-Gal4 driving UAS-CsChrimson (green). Neuropil is labelled with nc82 (magenta).

Biorbyt Ltd.
7 Signet Court, Swann Road
Cambridge
CB5 8LA
United Kingdom
Email: info@biorbyt.com, support@biorbyt.com
Phone: +44 (0)1223 859353 | Fax: +1 (415) 651-8558

Biorbyt LLC
68 TW Alexander Drive
Research Triangle Park
Durham
NC 27713-2847
United States
Email: info@biorbyt.com, support@biorbyt.com
Phone: +1 (415) 906-5211 | Fax: +1 (415) 651-8558

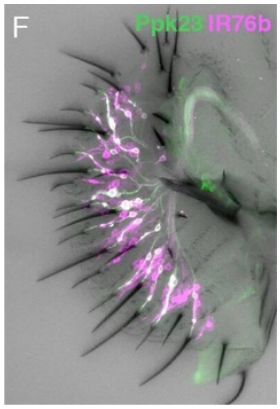

Molecular mapping of characterized and uncharacterized labellar GRN types.(A) Labellum expression of Ppk23-Gal4 restricted with ChAT-Gal80. Arrow indicates an S-type sensillum with two Ppk23 +GRNs, indicating incomplete elimination of Ppk23chat expression. (B) Ppk23-Gal4 (magenta) and Ppk23-LexA (green) label nearly identical labellar GRN populations. (C–F) IR76b-Gal4 expression (magenta) in labella co-labelled with markers for different GRN populations (green): Ppk28-LexA (C), Gr64f-LexA (D), Gr66a-LexA (E), and Ppk23-LexA (F). (G) IR94e projections to the brain revealed by IR94e-Gal4 driving UAS-CsChrimson (green). Neuropil is labelled with nc82 (magenta).

Biorbyt Ltd.
7 Signet Court, Swann Road
Cambridge
CB5 8LA
United Kingdom
Email: info@biorbyt.com, support@biorbyt.com
Phone: +44 (0)1223 859353 | Fax: +1 (415) 651-8558

Biorbyt LLC
68 TW Alexander Drive
Research Triangle Park
Durham
NC 27713-2847
United States
Email: info@biorbyt.com, support@biorbyt.com
Phone: +1 (415) 906-5211 | Fax: +1 (415) 651-8558

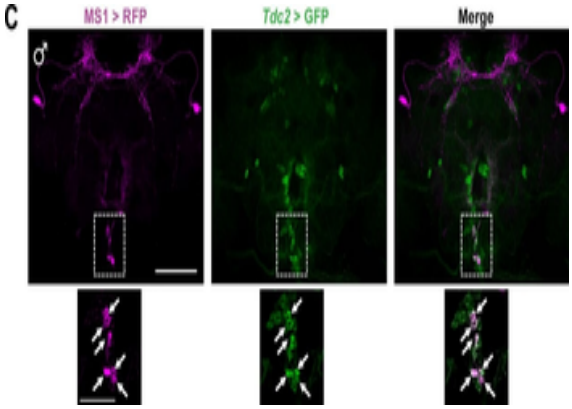

MS1 neurons in the SOG are octopaminergic.(A) Confocal projection of a whole-mounted MS1> CD8::GFP male (left) or female (right) adult central brain. Antibodies against GFP (green) and Bruchpilot (BRP, magenta) were used for immunostaining. Scale bar: 100 µm. (B) Confocal projection of the ventral nerve cord of a male or female expressing CD8::GFP under the control of MS1-Gal4. Scale bar: 50 µm. (C) Top: confocal projection of a male central brain expressing RFP (magenta) in MS1 neurons (using Gal4-UAS) and GFP (green) in Tdc2 neurons (using LexA-LexAOp). Scale bar: 100 µm. Bottom: Magnified view of the SOG region indicated by the rectangle in the corresponding image in the top row. Arrows point to neurons co-expressing MS1>RFP and Tdc2>GFP. Scale bar: 50 µm. (D) Expression of NaChBac::GFP in all MS1 neurons (left, MS1-Gal4, Tdc2-LexA/UAS-NaChBac) and in the non-octopaminergic subset (right, MS1-Gal4, Tdc2-LexA/UAS-NaChBac; LexAop-Gal80). Expression of Gal80, a suppressor of Gal4, in TDC2 neurons removed NaChBac::GFP expression specifically in the SOG. Scale bar: 100 µm. (E) Sleep profile of male flies of the indicated genotypes. N = 75–78. (F) Sleep profile of males in which MS1 neurons were activated with TrpA1 expression at 28°C in an iso31 control (left), Tbhnm18 mutant (middle), or Oamb286 mutant (right) background. N = 20–165. One-way ANOVA followed by Dunnett post hoc test relative to MS1>NaChBac, Tdc2-LexA/+ flies (E) or both parental controls (F).

Biorbyt Ltd.
7 Signet Court, Swann Road
Cambridge
CB5 8LA
United Kingdom
Email: info@biorbyt.com, support@biorbyt.com
Phone: +44 (0)1223 859353 | Fax: +1 (415) 651-8558

Biorbyt LLC
68 TW Alexander Drive
Research Triangle Park
Durham
NC 27713-2847
United States
Email: info@biorbyt.com, support@biorbyt.com
Phone: +1 (415) 906-5211 | Fax: +1 (415) 651-8558

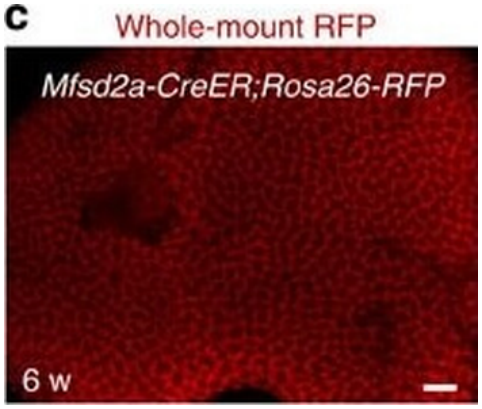

PP hepatocytes labelled by Mfsd2a-CreER.Schematic figures showing (a) our knock-in strategy for Mfsd2a-CreER allele using CRISPR/Cas9 by homologous recombination and (b) genetic lineage tracing strategy for Mfsd2a+ hepatocytes by Cre-LoxP recombination in Mfsd2a+ hepatocytes. (c) Whole-mount fluorescence view of the adult liver from 6-week-old Mfsd2a-CreER;Rosa26-RFP mice. Tamoxifen was induced at 2 days before analysis. Scale bar, 1 mm. (d) Immunostaining for RFP, CK19 and HNF4a on liver sections shows Mfsd2a-expressing hepatocytes in PP zone (P). Scale bars, 100 μm. (e) Immunostaining for RFP, PECAM and 4, 6-diamidino-2-phenylindole (DAPI) on liver sections shows Mfsd2a-expressing hepatocytes in the PP zone but not PC zone (*). Scale bars, 100 μm. (f) Isolation of RFP− and RFP+ cells by flow cytometry followed by quantitative RT–PCR (qRT–PCR) analysis for expression of RFP and Mfsd2a. Expression level of genes in the RFP− cells was set as 1. Error bars are s.e.m. of the mean for all the quantification in this study. (g) Expression of PP and PC genes detected by qRT–PCR. The x axis denotes RFP− (black) and RFP+ (red) groups, and the y axis denotes fold induction. *P 0.05; n = 3, two-tailed unpaired t-test. Each immunostaining image is a representative of four individual samples.

Biorbyt Ltd.
7 Signet Court, Swann Road
Cambridge
CB5 8LA
United Kingdom
Email: info@biorbyt.com, support@biorbyt.com
Phone: +44 (0)1223 859353 | Fax: +1 (415) 651-8558

Biorbyt LLC
68 TW Alexander Drive
Research Triangle Park
Durham
NC 27713-2847
United States
Email: info@biorbyt.com, support@biorbyt.com
Phone: +1 (415) 906-5211 | Fax: +1 (415) 651-8558

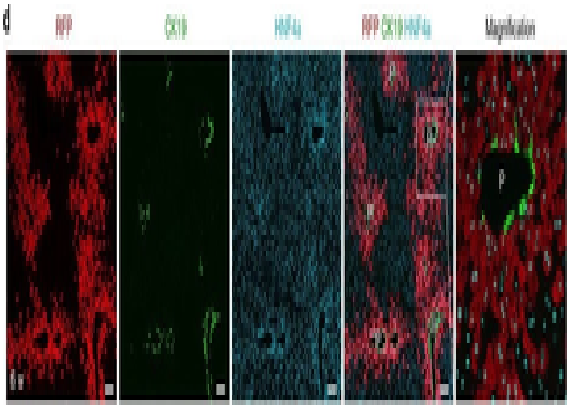

PP hepatocytes labelled by Mfsd2a-CreER.Schematic figures showing (a) our knock-in strategy for Mfsd2a-CreER allele using CRISPR/Cas9 by homologous recombination and (b) genetic lineage tracing strategy for Mfsd2a+ hepatocytes by Cre-LoxP recombination in Mfsd2a+ hepatocytes. (c) Whole-mount fluorescence view of the adult liver from 6-week-old Mfsd2a-CreER;Rosa26-RFP mice. Tamoxifen was induced at 2 days before analysis. Scale bar, 1 mm. (d) Immunostaining for RFP, CK19 and HNF4a on liver sections shows Mfsd2a-expressing hepatocytes in PP zone (P). Scale bars, 100 μm. (e) Immunostaining for RFP, PECAM and 4, 6-diamidino-2-phenylindole (DAPI) on liver sections shows Mfsd2a-expressing hepatocytes in the PP zone but not PC zone (*). Scale bars, 100 μm. (f) Isolation of RFP− and RFP+ cells by flow cytometry followed by quantitative RT–PCR (qRT–PCR) analysis for expression of RFP and Mfsd2a. Expression level of genes in the RFP− cells was set as 1. Error bars are s.e.m. of the mean for all the quantification in this study. (g) Expression of PP and PC genes detected by qRT–PCR. The x axis denotes RFP− (black) and RFP+ (red) groups, and the y axis denotes fold induction. *P 0.05; n = 3, two-tailed unpaired t-test. Each immunostaining image is a representative of four individual samples.

Biorbyt Ltd.
7 Signet Court, Swann Road
Cambridge
CB5 8LA
United Kingdom
Email: info@biorbyt.com, support@biorbyt.com
Phone: +44 (0)1223 859353 | Fax: +1 (415) 651-8558

Biorbyt LLC
68 TW Alexander Drive
Research Triangle Park
Durham
NC 27713-2847
United States
Email: info@biorbyt.com, support@biorbyt.com
Phone: +1 (415) 906-5211 | Fax: +1 (415) 651-8558

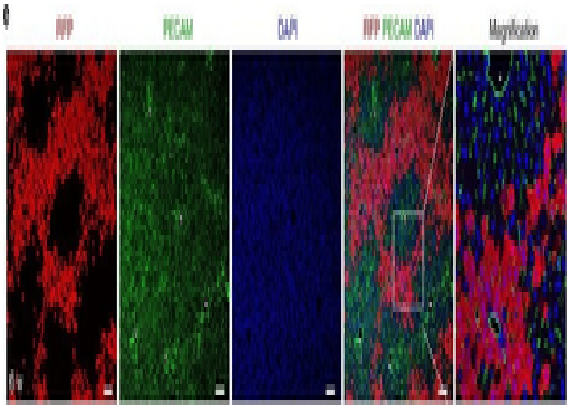

PP hepatocytes labelled by Mfsd2a-CreER.Schematic figures showing (a) our knock-in strategy for Mfsd2a-CreER allele using CRISPR/Cas9 by homologous recombination and (b) genetic lineage tracing strategy for Mfsd2a+ hepatocytes by Cre-LoxP recombination in Mfsd2a+ hepatocytes. (c) Whole-mount fluorescence view of the adult liver from 6-week-old Mfsd2a-CreER;Rosa26-RFP mice. Tamoxifen was induced at 2 days before analysis. Scale bar, 1 mm. (d) Immunostaining for RFP, CK19 and HNF4a on liver sections shows Mfsd2a-expressing hepatocytes in PP zone (P). Scale bars, 100 μm. (e) Immunostaining for RFP, PECAM and 4, 6-diamidino-2-phenylindole (DAPI) on liver sections shows Mfsd2a-expressing hepatocytes in the PP zone but not PC zone (*). Scale bars, 100 μm. (f) Isolation of RFP− and RFP+ cells by flow cytometry followed by quantitative RT–PCR (qRT–PCR) analysis for expression of RFP and Mfsd2a. Expression level of genes in the RFP− cells was set as 1. Error bars are s.e.m. of the mean for all the quantification in this study. (g) Expression of PP and PC genes detected by qRT–PCR. The x axis denotes RFP− (black) and RFP+ (red) groups, and the y axis denotes fold induction. *P 0.05; n = 3, two-tailed unpaired t-test. Each immunostaining image is a representative of four individual samples.

Biorbyt Ltd.
7 Signet Court, Swann Road
Cambridge
CB5 8LA
United Kingdom
Email: info@biorbyt.com, support@biorbyt.com
Phone: +44 (0)1223 859353 | Fax: +1 (415) 651-8558

Biorbyt LLC
68 TW Alexander Drive
Research Triangle Park
Durham
NC 27713-2847
United States
Email: info@biorbyt.com, support@biorbyt.com
Phone: +1 (415) 906-5211 | Fax: +1 (415) 651-8558

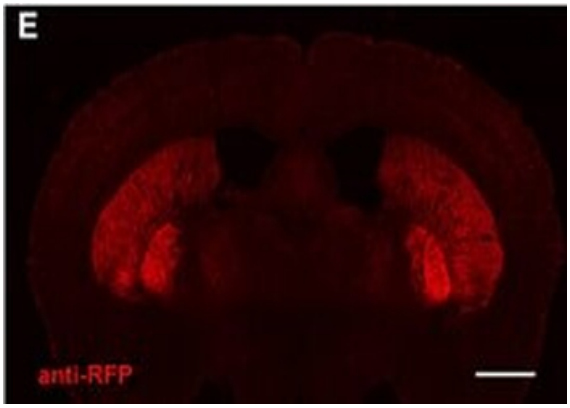

Preserved cell-type specific expression patterns in BAC transgenic mice created with advanced recombineering strategies. (A–D) Anti-2A slice staining in brain slices from DAT-ChETA line 3 mice reveals the distribution of membrane-targeted ChETA protein. Sagittal (A) and coronal (B) sections showing ChR2 expression in midbrain dopamine neurons. (C, D) High magnification images of axon terminal labeling in the dorsal striatum (C) and labeled neurons in the ventral tegmental area (D). (E, F) Anti-RFP slice staining in brain slices from A2A-ChETA line 13 mice showing tdTomato expression in striatopallidal medium spiny neurons (MSNs) in coronal (E) and sagittal (F) sections. Lighter expression can also be detected in putative cortical astrocytes. (G) Anti-2A slice staining in a sagittal brain slice from D1-ChETA line 1 mice showing ChETA expression in striatonigral MSNs. Additional expression is apparent in other brain regions, particularly the dentate gyrus, layer VI cortex, and olfactory bulb. (F) Anti-DARPP32 slice staining to label both striatonigral and striatopallidal MSNs. Scale bars: 1 mm in (A, B, E–H) and 100 µm in (C, D).

Biorbyt Ltd.
7 Signet Court, Swann Road
Cambridge
CB5 8LA
United Kingdom
Email: info@biorbyt.com, support@biorbyt.com
Phone: +44 (0)1223 859353 | Fax: +1 (415) 651-8558

Biorbyt LLC
68 TW Alexander Drive
Research Triangle Park
Durham
NC 27713-2847
United States
Email: info@biorbyt.com, support@biorbyt.com
Phone: +1 (415) 906-5211 | Fax: +1 (415) 651-8558

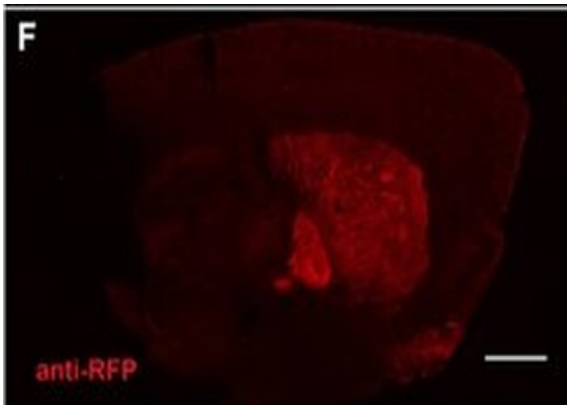

Preserved cell-type specific expression patterns in BAC transgenic mice created with advanced recombineering strategies. (A–D) Anti-2A slice staining in brain slices from DAT-ChETA line 3 mice reveals the distribution of membrane-targeted ChETA protein. Sagittal (A) and coronal (B) sections showing ChR2 expression in midbrain dopamine neurons. (C, D) High magnification images of axon terminal labeling in the dorsal striatum (C) and labeled neurons in the ventral tegmental area (D). (E, F) Anti-RFP slice staining in brain slices from A2A-ChETA line 13 mice showing tdTomato expression in striatopallidal medium spiny neurons (MSNs) in coronal (E) and sagittal (F) sections. Lighter expression can also be detected in putative cortical astrocytes. (G) Anti-2A slice staining in a sagittal brain slice from D1-ChETA line 1 mice showing ChETA expression in striatonigral MSNs. Additional expression is apparent in other brain regions, particularly the dentate gyrus, layer VI cortex, and olfactory bulb. (F) Anti-DARPP32 slice staining to label both striatonigral and striatopallidal MSNs. Scale bars: 1 mm in (A, B, E–H) and 100 µm in (C, D).

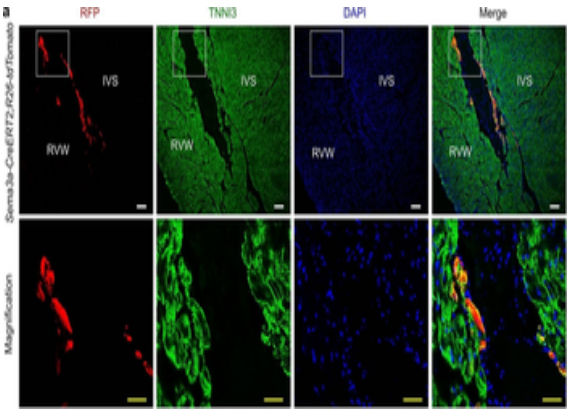

Quantification of the numbers of Sema3a+ cardiomyocytes in the adult heart. (a) Immunostaining for RFP and TNNI3 on adult heart sections. IVS, interventricular septum; RVW, right ventricular wall. Scale bars: white, 100 µm; yellow, 50 µm. (b) Image of isolated cardiomyocytes from the adult Sema3a CreERT2; R26-tdtomato heart showed Sema3a+ cardiomyocytes. (c) Quantification of the percentages of RFP+ cardiomyocytes in the heart sections. (d) Quantification of the percentages of RFP+ cells from among isolated cardiomyocytes. Each image is representative of 5 individual samples.

Biorbyt Ltd.
7 Signet Court, Swann Road
Cambridge
CB5 8LA
United Kingdom
Email: info@biorbyt.com, support@biorbyt.com
Phone: +44 (0)1223 859353 | Fax: +1 (415) 651-8558

Biorbyt LLC
68 TW Alexander Drive
Research Triangle Park
Durham
NC 27713-2847
United States
Email: info@biorbyt.com, support@biorbyt.com
Phone: +1 (415) 906-5211 | Fax: +1 (415) 651-8558

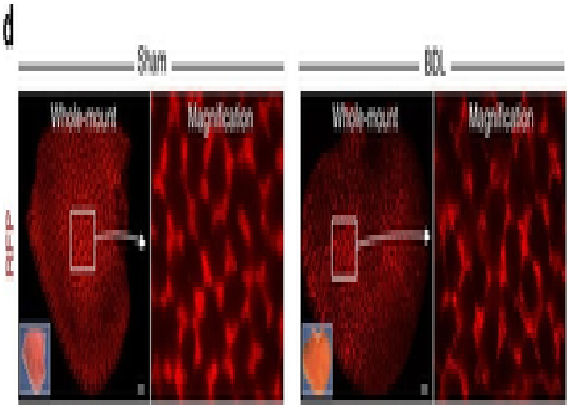

Reduction of pre-labelled PP hepatocytes after injury induced by BDL.(a) Schematic figure showing strategies for PP hepatocytes labelling and injury model induced by BDL. (b) Whole-mount bright view of sham and BDL livers. Scale bars, 2 mm. (c) Sirius red staining of liver sections. Scale bars, 200 µm. (d) Whole-mount fluorescence view of sham and BDL livers. Inserts are bright-field images of the same liver. Scale bars, 500 µm. (e) Immunostaining for RFP, CK19 and HNF4a on sham or BDL liver sections. Boxed regions are magnified in lower panels. Insertions indicate the quantification of the percentage of RFP+ hepatocytes in sham or BDL livers. n = 4. Error bars are s.e.m. of the mean. Scale bars, 500 µm. Each image is a representative of four individual samples.

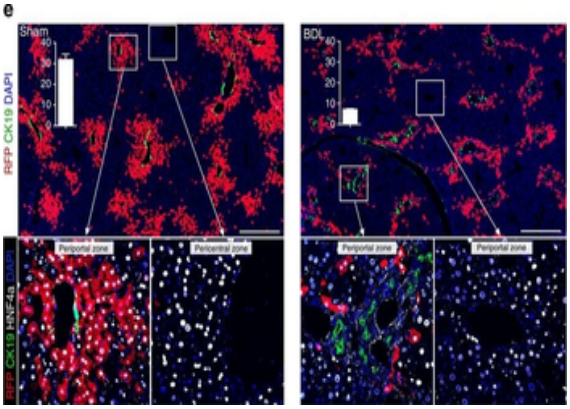

Reduction of pre-labelled PP hepatocytes after injury induced by BDL.(a) Schematic figure showing strategies for PP hepatocytes labelling and injury model induced by BDL. (b) Whole-mount bright view of sham and BDL livers. Scale bars, 2 mm. (c) Sirius red staining of liver sections. Scale bars, 200 µm. (d) Whole-mount fluorescence view of sham and BDL livers. Inserts are bright-field images of the same liver. Scale bars, 500 µm. (e) Immunostaining for RFP, CK19 and HNF4a on sham or BDL liver sections. Boxed regions are magnified in lower panels. Insertions indicate the quantification of the percentage of RFP+ hepatocytes in sham or BDL livers. n = 4. Error bars are s.e.m. of the mean. Scale bars, 500 µm. Each image is a representative of four individual samples.

Biorbyt Ltd.
7 Signet Court, Swann Road
Cambridge
CB5 8LA
United Kingdom
Email: info@biorbyt.com, support@biorbyt.com
Phone: +44 (0)1223 859353 | Fax: +1 (415) 651-8558

Biorbyt LLC
68 TW Alexander Drive
Research Triangle Park
Durham
NC 27713-2847
United States
Email: info@biorbyt.com, support@biorbyt.com
Phone: +1 (415) 906-5211 | Fax: +1 (415) 651-8558

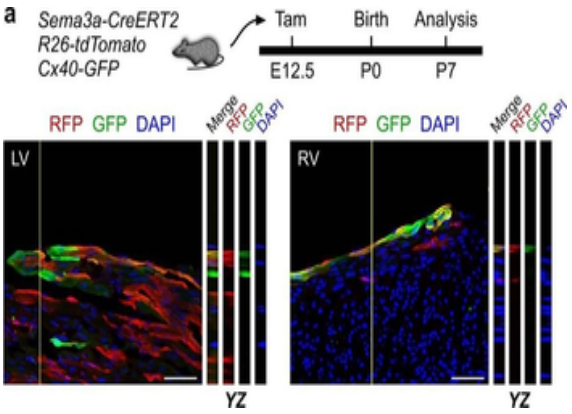

Specialization of Sema3a+ cardiomyocytes into the conduction system in the developing heart. (a–f) Z-stack images of RFP and GFP immunostaining on Sema3a-CreERT2; R26-tdTomato; Cx40-GFP heart sections. Tamoxifen was administered at E12.5 (a, b), E14.5 (c, d) and E18.5 (e, f). The hearts were collected at P7 and P21 for each group. YZ indicates signals from the dotted lines on the Z-stack images. Scale bars, 50 µm. Each image is representative of 5 individual samples. (g) Schematic figure showing Sema3a+ cells (red) and CX40+ cells (green) in the developing and adult heart.

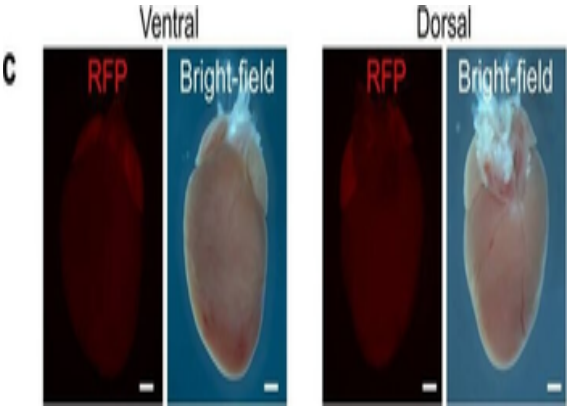

The adult expression map of Sema3a in the heart. (a) Schematic showing the crossing of the mice to generate the Sema3a-CreERT2; R26-tdTomato mice. (b) Genetic labelling of the Sema3a+ cells via tamoxifen administration. (c) Whole-mount fluorescence and bright-field views of a Sema3a-CreERT2; R26-tdTomato mouse heart. (d) Immunostaining for RFP and TNNI3 on a Sema3a-CreERT2; R26-tdTomato heart section showing the rarity of RFP+ cells in the atrium. LA, left atrium. (e) No Sema3a+ cells were detected in the SA node. (f) The expression of Sema3a in the AV node. (g) Immunostaining for RFP, GFP and TNNI3 in a Sema3a-CreERT2; R26-tdTomato; Cx40-GFP mouse heart section showing that the CX40+ coronary artery (arrowhead) was negative for RFP. (h) Whole-mount fluorescence view of a Sema3a-CreERT2; R26-tdTomato; Cx40-GFP mouse heart. LBB, left bundle branch; LPF, left Purkinje fibre; IVS, interventricular septum; LVW, left ventricular free wall. The dotted line indicates the limits between the IVS and the LVW. (i) Immunostaining for RFP and GFP on heart sections of a Sema3a-CreERT2; R26-tdTomato; Cx40-GFP mouse. Sema3a was not detected in the LBB or RBB, which were positive for Cx40-GFP. (j) Z-stack confocal image showing that Sema3a was expressed in the Purkinje fibres. XZ and YZ indicate the signals from the dotted lines on the Z-stack images in (j). Scale bars, 1 mm in (c) 500 µm in (e, g, h) and 100 µm in (d, f, i) and (j). Each image is representative of 5 individual samples.

Biorbyt Ltd.
7 Signet Court, Swann Road
Cambridge
CB5 8LA
United Kingdom
Email: info@biorbyt.com, support@biorbyt.com
Phone: +44 (0)1223 859353 | Fax: +1 (415) 651-8558

Biorbyt LLC
68 TW Alexander Drive
Research Triangle Park
Durham
NC 27713-2847
United States
Email: info@biorbyt.com, support@biorbyt.com
Phone: +1 (415) 906-5211 | Fax: +1 (415) 651-8558

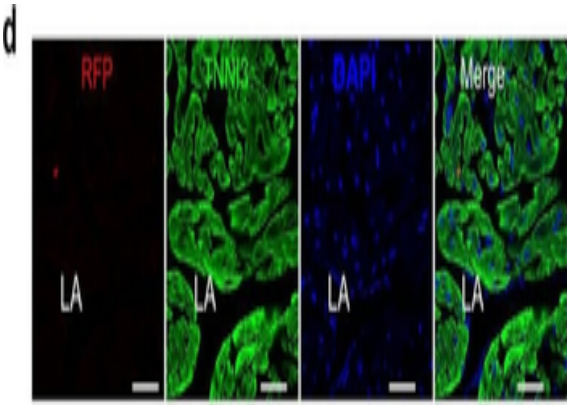

The adult expression map of Sema3a in the heart. (a) Schematic showing the crossing of the mice to generate the Sema3a-CreERT2; R26-tdTomato mice. (b) Genetic labelling of the Sema3a+ cells via tamoxifen administration. (c) Whole-mount fluorescence and bright-field views of a Sema3a-CreERT2; R26-tdTomato mouse heart. (d) Immunostaining for RFP and TNNI3 on a Sema3a-CreERT2; R26-tdTomato heart section showing the rarity of RFP+ cells in the atrium. LA, left atrium. (e) No Sema3a+ cells were detected in the SA node. (f) The expression of Sema3a in the AV node. (g) Immunostaining for RFP, GFP and TNNI3 in a Sema3a-CreERT2; R26-tdTomato; Cx40-GFP mouse heart section showing that the CX40+ coronary artery (arrowhead) was negative for RFP. (h) Whole-mount fluorescence view of a Sema3a-CreERT2; R26-tdTomato; Cx40-GFP mouse heart. LBB, left bundle branch; LPF, left Purkinje fibre; IVS, interventricular septum; LVW, left ventricular free wall. The dotted line indicates the limits between the IVS and the LVW. (i) Immunostaining for RFP and GFP on heart sections of a Sema3a-CreERT2; R26-tdTomato; Cx40-GFP mouse. Sema3a was not detected in the LBB or RBB, which were positive for Cx40-GFP. (j) Z-stack confocal image showing that Sema3a was expressed in the Purkinje fibres. XZ and YZ indicate the signals from the dotted lines on the Z-stack images in (j). Scale bars, 1 mm in (c) 500 µm in (e, g, h) and 100 µm in (d, f, i) and (j). Each image is representative of 5 individual samples.

Biorbyt Ltd.
7 Signet Court, Swann Road
Cambridge
CB5 8LA
United Kingdom
Email: info@biorbyt.com, support@biorbyt.com
Phone: +44 (0)1223 859353 | Fax: +1 (415) 651-8558

Biorbyt LLC
68 TW Alexander Drive
Research Triangle Park
Durham
NC 27713-2847
United States
Email: info@biorbyt.com, support@biorbyt.com
Phone: +1 (415) 906-5211 | Fax: +1 (415) 651-8558

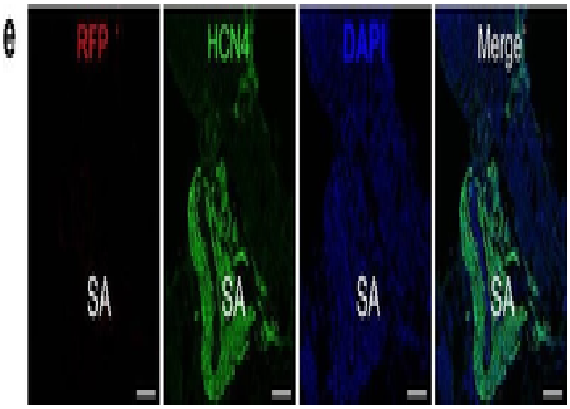

The adult expression map of Sema3a in the heart. (a) Schematic showing the crossing of the mice to generate the Sema3a-CreERT2; R26-tdTomato mice. (b) Genetic labelling of the Sema3a+ cells via tamoxifen administration. (c) Whole-mount fluorescence and bright-field views of a Sema3a-CreERT2; R26-tdTomato mouse heart. (d) Immunostaining for RFP and TNNI3 on a Sema3a-CreERT2; R26-tdTomato heart section showing the rarity of RFP+ cells in the atrium. LA, left atrium. (e) No Sema3a+ cells were detected in the SA node. (f) The expression of Sema3a in the AV node. (g) Immunostaining for RFP, GFP and TNNI3 in a Sema3a-CreERT2; R26-tdTomato; Cx40-GFP mouse heart section showing that the CX40+ coronary artery (arrowhead) was negative for RFP. (h) Whole-mount fluorescence view of a Sema3a-CreERT2; R26-tdTomato; Cx40-GFP mouse heart. LBB, left bundle branch; LPF, left Purkinje fibre; IVS, interventricular septum; LVW, left ventricular free wall. The dotted line indicates the limits between the IVS and the LVW. (i) Immunostaining for RFP and GFP on heart sections of a Sema3a-CreERT2; R26-tdTomato; Cx40-GFP mouse. Sema3a was not detected in the LBB or RBB, which were positive for Cx40-GFP. (j) Z-stack confocal image showing that Sema3a was expressed in the Purkinje fibres. XZ and YZ indicate the signals from the dotted lines on the Z-stack images in (j). Scale bars, 1 mm in (c) 500 µm in (e, g, h) and 100 µm in (d, f, i) and (j). Each image is representative of 5 individual samples.

Biorbyt Ltd.
7 Signet Court, Swann Road
Cambridge
CB5 8LA
United Kingdom
Email: info@biorbyt.com, support@biorbyt.com
Phone: +44 (0)1223 859353 | Fax: +1 (415) 651-8558

Biorbyt LLC
68 TW Alexander Drive
Research Triangle Park
Durham
NC 27713-2847
United States
Email: info@biorbyt.com, support@biorbyt.com
Phone: +1 (415) 906-5211 | Fax: +1 (415) 651-8558

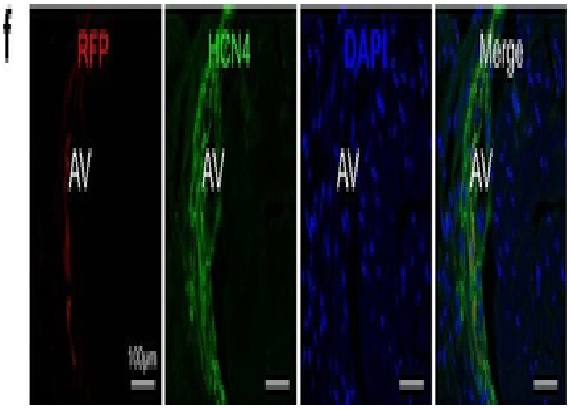

The adult expression map of Sema3a in the heart. (a) Schematic showing the crossing of the mice to generate the Sema3a-CreERT2; R26-tdTomato mice. (b) Genetic labelling of the Sema3a+ cells via tamoxifen administration. (c) Whole-mount fluorescence and bright-field views of a Sema3a-CreERT2; R26-tdTomato mouse heart. (d) Immunostaining for RFP and TNNI3 on a Sema3a-CreERT2; R26-tdTomato heart section showing the rarity of RFP+ cells in the atrium. LA, left atrium. (e) No Sema3a+ cells were detected in the SA node. (f) The expression of Sema3a in the AV node. (g) Immunostaining for RFP, GFP and TNNI3 in a Sema3a-CreERT2; R26-tdTomato; Cx40-GFP mouse heart section showing that the CX40+ coronary artery (arrowhead) was negative for RFP. (h) Whole-mount fluorescence view of a Sema3a-CreERT2; R26-tdTomato; Cx40-GFP mouse heart. LBB, left bundle branch; LPF, left Purkinje fibre; IVS, interventricular septum; LVW, left ventricular free wall. The dotted line indicates the limits between the IVS and the LVW. (i) Immunostaining for RFP and GFP on heart sections of a Sema3a-CreERT2; R26-tdTomato; Cx40-GFP mouse. Sema3a was not detected in the LBB or RBB, which were positive for Cx40-GFP. (j) Z-stack confocal image showing that Sema3a was expressed in the Purkinje fibres. XZ and YZ indicate the signals from the dotted lines on the Z-stack images in (j). Scale bars, 1 mm in (c) 500 µm in (e, g, h) and 100 µm in (d, f, i) and (j). Each image is representative of 5 individual samples.

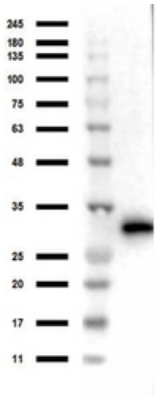

Western Blot of Rabbit anti-RFP Antibody. Lane 1: Opal Prestained Marker. Lane 2: 50 ng of RFP. Primary Antibody: Anti-RFP at 1 µg/ml overnight at 2-8°C. Secondary Antibody: Goat anti-Rabbit HRP (p/n orb347654) at 1:70000 for 30 mins at RT. Block: BlockOut Universal blocking buffer (p/n orb348644). Expect ~27kDa.

Biorbyt Ltd.
7 Signet Court, Swann Road
Cambridge
CB5 8LA
United Kingdom
Email: info@biorbyt.com, support@biorbyt.com
Phone: +44 (0)1223 859353 | Fax: +1 (415) 651-8558

Biorbyt LLC
68 TW Alexander Drive
Research Triangle Park
Durham
NC 27713-2847
United States
Email: info@biorbyt.com, support@biorbyt.com
Phone: +1 (415) 906-5211 | Fax: +1 (415) 651-8558

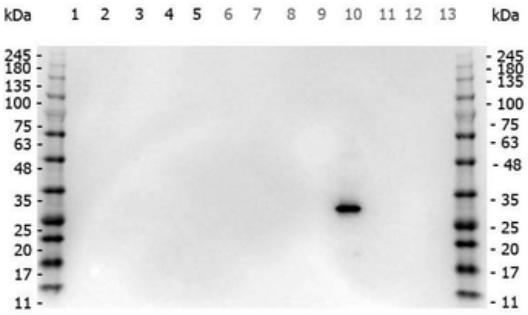

Western Blot of Rabbit anti-RFP antibody. Marker: Opal Pre-stained ladder. Lane 1: HEK293 lysate (p/n orb348669). Lane 2: HeLa Lysate (p/n orb348668). Lane 3: CHO/K1 Lysate. Lane 4: MDA-MB-231 (p/n orb348700). Lane 5: A431 Lysate (p/n orb348665). Lane 6: Jurkat Lysate (p/n orb348674). Lane 7: NIH/3T3 Lysate (p/n orb348714). Lane 8: E-coli HCP Control (p/n orb342262). Lane 9: FLAG Positive Control Lysate (p/n orb348661). Lane 10: Red Fluorescent Protein (p/n orb345960). Lane 11: Green Fluorescent Protein (p/n orb345957). Lane 12: Glutathione-S-Transferase Protein. Lane 13: Maltose Binding Protein. Load: 10 µg of lysate or 50 ng of purified protein per lane. Primary antibody: RFP antibody at 1 ug/ml overnight at 4C. Secondary antibody: Peroxidase rabbit secondary antibody (p/n orb347654) at 1:30000 for 60 min at RT. Blocking Buffer: 1% Casein-TTBS for 30 min at RT. Predicted/Observed size: 30 kDa for RFP.

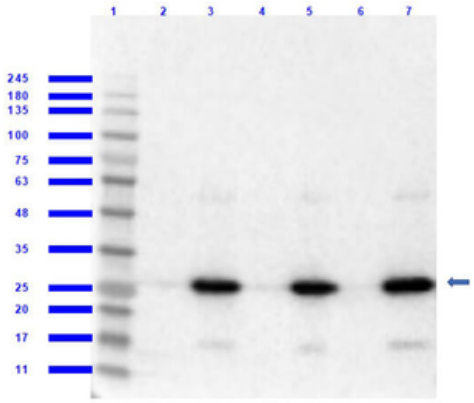

Western Blot of Rabbit Anti-RFP MW Hu, Ms, Rt Antibody. Lane 1: Opal Prestained Molecular Weight Marker. Lane 2: RFP/HEK293T WCL [0.05/10 µg] [+]. Lane 3: HEK293T Whole Cell Lysate [-]. Lane 4: RFP/NIH/3T3 Whole Cell Lysate (p/n orb345960/orb348714) [0.05/10 µg] [+]. Lane 5: NIH/3T3 Whole Cell Lysate [-]. Lane 6: RFP/PC-12 Whole Cell Lysate (p/n orb345960/orb348733) [0.05/10 µg] [+]. Lane 7: PC-12 Whole Cell Lysate [-]. Primary Antibody: Anti-RFP at 1:1000 overnight at 2-8°C. Secondary Antibody: Goat Anti-Rabbit IgG Peroxidase (p/n orb347654) at 1:70000 at RT for 30 mins. Predicted/Observed MW: ~27kDa. Exposure: 2 sec.

Biorbyt Ltd.
7 Signet Court, Swann Road
Cambridge
CB5 8LA
United Kingdom
Email: info@biorbyt.com, support@biorbyt.com
Phone: +44 (0)1223 859353 | Fax: +1 (415) 651-8558

Biorbyt LLC
68 TW Alexander Drive
Research Triangle Park
Durham
NC 27713-2847
United States
Email: info@biorbyt.com, support@biorbyt.com
Phone: +1 (415) 906-5211 | Fax: +1 (415) 651-8558

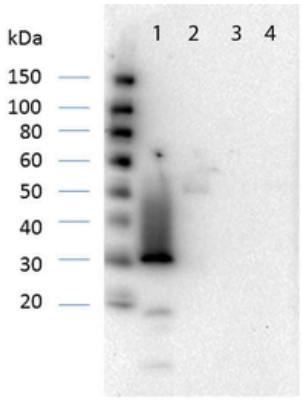

Western Blot of RFP Antibody Pre-Absorbed. Lane 1: RFP (p/n orb345960). Lane 2: Human IgG (p/n orb346219). Lane 3: Goat IgG (p/n orb2652767). Lane 4: Mouse IgG (p/n orb2652749). Load: 50 ng per lane. Primary antibody: RFP Antibody Pre-Absorbed at 1:1000 overnight at 4°C. Secondary antibody: Peroxidase conjugated rabbit secondary antibody (p/n orb347654) at 1:40000 for 30 min at RT. Block: orb348637 Blocking Buffer for 30 min at RT. Predicted/Observed size: 27 kDa, 30 kDa.

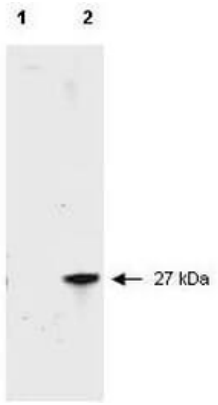

Western blot of RFP recombinant protein detected with Biorbyt's polyclonal anti-RFP antibody. Lane 1 shows no reaction against a GFP recombinant protein present in 10 µg of HeLa cell extract. Lane 2 shows a single band detected in 10 µg of a HeLa lysate containing RFP recombinant protein as a 27 kDa band. A 4-12% Bis-Tris gradient gel (Invitrogen) was used for SDS-PAGE. The membrane was blocked and then probed with Anti-RFP diluted 1:2500 for 1 h at RT followed by washes and reaction with a 1:5000 dilution of IRDye™800 conjugated Goat-a-Rabbit IgG [H&L] MX.

Biorbyt Ltd.
7 Signet Court, Swann Road
Cambridge
CB5 8LA
United Kingdom
Email: info@biorbyt.com, support@biorbyt.com
Phone: +44 (0)1223 859353 | Fax: +1 (415) 651-8558

Biorbyt LLC
68 TW Alexander Drive
Research Triangle Park
Durham
NC 27713-2847
United States
Email: info@biorbyt.com, support@biorbyt.com
Phone: +1 (415) 906-5211 | Fax: +1 (415) 651-8558

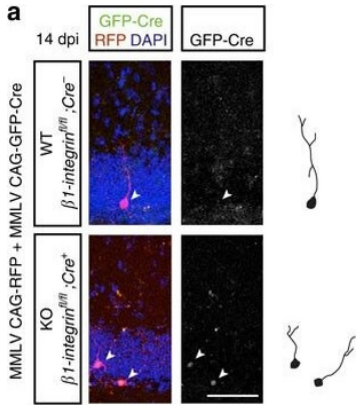

β1-integrins are required for dendritic growth and spine development in adult-born DG granule cells.(a, d) The dentate gyrus of β1-integrinfl/fl mice was injected with MMLV CAG-RFP and MMLV CAG-GFP-Cre and immunostained for RFP and GFP at 14 or 56 days post-injection (dpi). Despite underestimation of the dendritic length and complexity due to low expression of RFP at 14 dpi, cell-autonomous ablation of β1-integrin in GFP-positive, RFP-positive cells induces a clear reduction in dendritic morphology at 14 dpi. DAPI is shown in blue. WT, GFP-negative, RFP-positive cell; KO, GFP-positive, RFP-positive cell. Right panels depict representative tracings based on confocal z-stack images. (b, e) Quantification of dendritic length and number of branch points in WT (black bars, n = 4) and KO (green bars, n = 4) littermates (two-way ANOVA, post-hoc t-test, 56 dpi: P = 0.176 and P = 0.336). (c, f) Sholl-analysis of the dendritic tree of WT (black dashed-lines) and KO cells (green lines). Dendritic length per radius distance from soma (30 µm radius interval) was decreased in KO adult-born granule cells (nGCs) (14 dpi: n = 20 WT cells/4 mice, n = 9 KO cells/4 mice, 56 dpi: n = 27 WT cells/4 mice, n = 20 KO cells/4 mice. Repeated-measures ANOVA 14 dpi: F(7, 175) = 2.625, 56 dpi: F(9, 405) = 0.724, P = 0.533). (g) Schematic representation of the DG indicating the regions selected for spine density quantification. IML, inner molecular layer; OML, outer molecular layer. (h) Representative images showing spine-bearing dendritic segments in the OML and the IML in WT and KO nGCs. (i) Quantification of spine density on nGCs at 56 dpi reveals differences between WT (n = 4) and KO (n = 4) granule cells (two-way ANOVA, post-hoc t-test). Data are represented as means±s.e.m. *P 0.05 and **P 0.01. Scale bars: (a, d) 25 µm; (h) 10 µm.

Biorbyt Ltd.
7 Signet Court, Swann Road
Cambridge
CB5 8LA
United Kingdom
Email: info@biorbyt.com, support@biorbyt.com
Phone: +44 (0)1223 859353 | Fax: +1 (415) 651-8558

Biorbyt LLC
68 TW Alexander Drive
Research Triangle Park
Durham
NC 27713-2847
United States
Email: info@biorbyt.com, support@biorbyt.com
Phone: +1 (415) 906-5211 | Fax: +1 (415) 651-8558

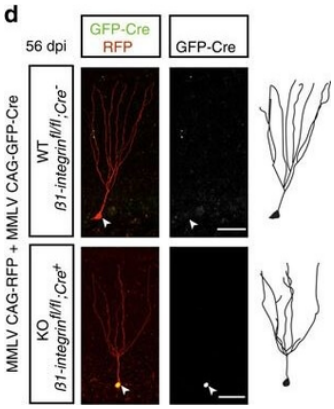

β1-integrins are required for dendritic growth and spine development in adult-born DG granule cells.(a, d) The dentate gyrus of β1-integrinfl/fl mice was injected with MMLV CAG-RFP and MMLV CAG-GFP-Cre and immunostained for RFP and GFP at 14 or 56 days post-injection (dpi). Despite underestimation of the dendritic length and complexity due to low expression of RFP at 14 dpi, cell-autonomous ablation of β1-integrin in GFP-positive, RFP-positive cells induces a clear reduction in dendritic morphology at 14 dpi. DAPI is shown in blue. WT, GFP-negative, RFP-positive cell; KO, GFP-positive, RFP-positive cell. Right panels depict representative tracings based on confocal z-stack images. (b, e) Quantification of dendritic length and number of branch points in WT (black bars, n = 4) and KO (green bars, n = 4) littermates (two-way ANOVA, post-hoc t-test, 56 dpi: P = 0.176 and P = 0.336). (c, f) Sholl-analysis of the dendritic tree of WT (black dashed-lines) and KO cells (green lines). Dendritic length per radius distance from soma (30 µm radius interval) was decreased in KO adult-born granule cells (nGCs) (14 dpi: n = 20 WT cells/4 mice, n = 9 KO cells/4 mice, 56 dpi: n = 27 WT cells/4 mice, n = 20 KO cells/4 mice. Repeated-measures ANOVA 14 dpi: F(7, 175) = 2.625, 56 dpi: F(9, 405) = 0.724, P = 0.533). (g) Schematic representation of the DG indicating the regions selected for spine density quantification. IML, inner molecular layer; OML, outer molecular layer. (h) Representative images showing spine-bearing dendritic segments in the OML and the IML in WT and KO nGCs. (i) Quantification of spine density on nGCs at 56 dpi reveals differences between WT (n = 4) and KO (n = 4) granule cells (two-way ANOVA, post-hoc t-test). Data are represented as means±s.e.m. *P 0.05 and **P 0.01. Scale bars: (a, d) 25 µm; (h) 10 µm.

Biorbyt Ltd.
7 Signet Court, Swann Road
Cambridge
CB5 8LA
United Kingdom
Email: info@biorbyt.com, support@biorbyt.com
Phone: +44 (0)1223 859353 | Fax: +1 (415) 651-8558

Biorbyt LLC
68 TW Alexander Drive
Research Triangle Park
Durham
NC 27713-2847
United States
Email: info@biorbyt.com, support@biorbyt.com
Phone: +1 (415) 906-5211 | Fax: +1 (415) 651-8558